Collective Orderliness of Schooling Fish via Integrated Information Theory Considering Polar Nematic State

Shumpei Wakabayashi[1,2], **Kentaro Morikawa**[1], **Yuuki Maeda**[1], **and Yasuhiro Inoue**[1,*]

[1]The Department of Micro Engineering, Graduate School of Engineering, Kyoto University, Kyoto University Katsura C3 Building Nisshikyo-ku, Kyoto 615-8540, Japan
[2]Graduate School of Information Science and Technology, The University of Tokyo, 7-3-1 Hongo, Bunkyo-ku, Tokyo, 113-8656, Japan
[*]Correspondence and requests for materials should be addressed to Y.I. (email: inoue.yasuhiro.4n@kyoto-u.ac.jp)

ABSTRACT

In this study, we record video of the behaviors of schooling fish and analyze their collective motions. An individual fish is modeled as an anisotropic rod-like active matter. A "polar nematic" state refers to a system whose components tend to point in their long-axis direction but do not have positional order. Based on their state transition derived from the polar nematic model, the internal causal influences among parts of the system is calculated according to Integrated information theory (IIT). The resulting complex (Φ) is used as the order parameter. A polar nematic model with a strong anisotropy shows that Φ demonstrates a disorder-to-order transition between the groups of five and six fish. In contrast, the isotropic simple-interaction model developed in this study shows that the Φ metric is independent of the sample size. When employing mutual information (MI) as the order parameter instead of Φ, as the sample size increases, MI increases but a disorder-to-order transition does not occur. Based on the results of this study, we conclude that Φ reflects certain aspects of the internal state of a system that MI cannot capture.

Introduction

Various groups of organisms exhibit collective motion. Motion coordination at the system level is derived from lower-level interactions of its members or components. Observations of the overall order and structure of a group and the complex movements of its members give rise to the notion of self-organization[1]. This concept refers to pattern formation processes where an orderly structure emerges from a disorderly state through the interactions between individual members in the absence of external force or stimuli. In a self-organizing system, individual components tend to align their behaviors in response to those of their neighbors[2]. At the same time, they do not always match the behavior of others, which weaken the big direction of the group[3]. Currently, the behavioral synchrony and congruence that organisms often exhibit have many enigmas.

One of the earliest mathematical attempts to describe a collective biological behavior based on local interactions among group members is the boids (= bird + oids) model published in 1987, which simulated the behavior of a flock of birds[4,5]. To simulate flock dynamics, the boids model identified three key behavioral urges or local interactions of individuals. First, boids avoid collisions with nearby flockmates. Second, boids attempt to match their velocities with nearby flockmates. Third, boids attempt to remain close to nearby flockmates. Based on these assumptions, the boids model successfully simulated flock behavior, and attracted wide scientific attention. Building on these early models that evaluated the aggregate actions of individual animals, a new approach employing non-equilibrium statistical physics has attracted a surging attention[6]. In particular, the study of "active matter," or particles and objects that move spontaneously, is a rapidly growing discipline[7].

The Vicsek model is a famous mathematical description of active matter[8,9]. It is simpler than the boids model, and consists of a group of self-propelled individuals that move within given constraints. Specifically, an individual component is a point-like particle with a given velocity and heading direction. Each particle aligns its velocity and heading direction with those of its neighbors in the presence of noise. If the average velocity of the entire group is defined as the order parameter, the Vicsek model exhibits a disorder-to-order transition at a critical point as a function of the order parameter. The Vicsek model served as a springboard for a subsequent statistical physics study of collective biological motion [10].

An in-depth analysis of real-life collective motion revealed the limitations of the Vicsek model. For example,

research on a flock of starlings identified anisotropy in the motion direction[11] and a turning inertia against changing the curvature of the trajectory[12][13]. These findings represent complexities that go beyond the simple and symmetrical framework of the original Vicsek model and demonstrate that developing a model to accurately account for the complex and asymmetric nature of collective biological behaviors is a major challenge.

What variables represent the collective orderliness of a system? Because the concept of system collective orderliness is multi-dimensional, there is not a universal definition or measure. System collective orderliness must be described in a specific manner to be represented by a quantitative variable. In the original Vicsek model, the average particle velocity of the system was defined as the order parameter. In a separate approach, mutual information (MI), which is defined to quantify the maximum information of a system, may also be used as an order parameter[14]. In either situation, certain complex properties of the dynamic system under observation are used as the order parameter, although the intrinsic cause-effect structure of the system is not considered. Against this backdrop, a method has been developed to infer the hidden intra-system relationship based on the behaviors of individual components along the time axis. Integrated information theory (IIT) provides a mathematical framework to quantify the cause-effect powers of any given mechanism within a system from the system's intrinsic perspective rather than from an extrinsic perspective of an outside observer. IIT enables the system's intrinsic cause-effect structure, which is not measurable from the outside, to be characterized[15].

This research contributes to knowledge about active matter by constructing a model to describe the inter-relationship between the components constituting a biological system and quantifying the system's degree of collective orderliness. Here, we hypothesize that a mathematical model simulating the complex nature of the system components will demonstrate a disorder to-order transition as the number of system components increases. In addition to the simple and symmetric characteristics of the components such as distance and orientation, our model assumes anisotropic interactions such as those described in the mathematical models for polar nematic liquid crystals. Moreover, our model uses a complex (Φ) metric as the order parameter. This variable, which was originally developed in the IIT theory, represents the amount of intrinsic information of the system components. This study uses tropical freshwater fish, neon tetra (Paracheirodon innesi) due to their schooling behavior, hardiness, ease of keeping, and cost efficiency.

Modeling and Measurement Methods for Schooling Fish

Mathematical Modeling for the Polar Nematic System

First, we conceptually explain the proposed nematic model to describe the state of collective orderliness. Next, we provide a mathematical description of the electric dipole moment vector, which serves as the basis to construct the nematic model.

Polar Nematics

"Soft" matter refers to a class of materials such as polymers, liquid crystals, colloids, biological membranes, and biomolecules, whose structural and dynamic properties are an intermediate between those of highly ordered crystals and disordered fluids. Soft matter commonly has a complex multilayer structure with a high flexibility and a certain degree of freedom. When placed in a non-equilibrium environment, soft matter exhibits nonlinear non-equilibrium dynamics (active matter). Soft matter studies investigate the autonomy and functional hierarchy in living organisms. To model fish, we first considered the self-assembly of liquid crystals. Liquid crystals are a highly structured liquid where the constituent molecules are orientationally ordered but their centers of gravity lack positional order. Liquid crystals are composed of multiple rod-shaped molecules. They are typically classified into the three phases according to the molecular orientation and assembly[16]: cholesteric, smectic, and nematic. Here, we focus on nematic liquid crystals, which are characterized by the anisotropic orientation of their constituent molecules. Anisotropy typically refers to substances whose optical or other physical properties depend on their axis of orientation. Here this term denotes a directional dependence in a broader sense. In the nematic state, rod-like molecules align in their long-axis direction without positional order. The average long-axis orientation of the molecules is determined by the amount of energy due to its angular deviation from the direction of the optical axis or director. In addition, anisotropic attraction and repulsion forces help stabilize the liquid crystal state. The orientational order of nematic liquid crystals is temperature dependent and changes greatly near the nematic-isotropic phase transition temperature[17].

Similar to simulations of the behavior of liquid crystals, individual neon tetras are modeled using rod-shaped molecules. On the macroscopic level, neon tetras tend to orient in the same direction. On a local level, however, their orientations may fluctuate. Although nematic liquid crystals generally do not show polarity along the long axis, polarity along the long axis of the model molecule is assumed to simulate the forward movement of the fish. Specifically, our nematic model for fish schooling consists of polar anisotropic molecules, which show orientational

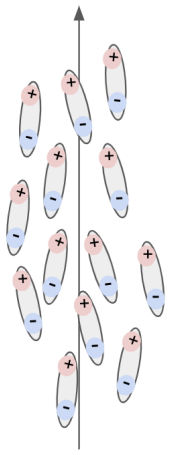

Figure 1. Polar nematic state : The arrangement of rod-like molecules is aligned in the long axis direction, but the neighbors are irregular

order along the long axis but not positional order (Figure 1)

The polar nematic state can be modeled using electric dipole moment vectors and anisotropic dipole-dipole interactions. The next section introduces a mathematical formula to describe the energy state of an individual molecule i in the polar nematic state using electric dipole moment vectors.

Electric Dipole Moment Vectors and Anisotropic Dipole-Dipole Interactions

When a pair of point charges ($\pm q$) are separated by a distance s, and the vector from the $-q$ charge to the $+q$ charge is designated as $\boldsymbol{s}$, the electric dipole moment vector $\boldsymbol{p}$ is expressed as[18,19]

$$\boldsymbol{p} = q\boldsymbol{s} \tag{1}$$

Assuming that the electric dipole moment vectors at positions $\boldsymbol{R_i}$ and $\boldsymbol{R_j}$ $(= \boldsymbol{R_i} + \boldsymbol{r_{ij}})$ are $\boldsymbol{p_i}$ and $\boldsymbol{p_j}$, respectively, then the electric field created at position $\boldsymbol{R_j}$ by the electric dipole moment vector $\boldsymbol{p_i}$ is expressed by employing the dipole approximation as

$$\mathbf{E}(\boldsymbol{R_j}) = \frac{3\left(\boldsymbol{p_i}\cdot\boldsymbol{r_{ij}}\right)\boldsymbol{r_{ji}} - \boldsymbol{p}r^2}{r^5} \tag{2}$$

Considering that the potential energy at position $\boldsymbol{p_j}$ due to the electric field created by $\boldsymbol{p_i}$ is expressed as $v = -\boldsymbol{p_j}\cdot\mathbf{E}(\boldsymbol{R_j})$, the above equation can be transformed into

$$v = \frac{\left(\boldsymbol{p_i}\cdot\boldsymbol{p_j}\right)r^2 - 3\left(\boldsymbol{p_i}\cdot\boldsymbol{r_{ij}}\right)\left(\boldsymbol{p_j}\cdot\boldsymbol{r_{ji}}\right)}{r^5} \tag{3}$$

Consider that the electric moment vector $\boldsymbol{p_i}$ represents a molecule i. Assuming that $\boldsymbol{n_i}$ represents the orientation of the molecule i and $\sqrt{C_i}$ is an appropriate constant, then $\boldsymbol{p_i}$ is given as

$$\boldsymbol{p_i} = \sqrt{C_i}\boldsymbol{n_i} \tag{4}$$

A similar process is implemented for $\boldsymbol{p_j}$ of another molecule j. If the properties of individual molecules are the same, then $C_i = C_j$. Applying a generic constant $\sqrt{C}$ to Equation (4) gives the following generalized formula

$$\boldsymbol{p_i} = \sqrt{C}\boldsymbol{n_i} \tag{5}$$

Now, the potential energy of a molecule i attributable to the electric dipole moment vector $\boldsymbol{p_j}$ is designated as

$$g_v\left(\boldsymbol{n_i},\boldsymbol{n_j},\boldsymbol{r_{ij}}\right) = \frac{C}{r^3}\left\{\boldsymbol{n_i}\cdot\boldsymbol{n_j} - 3\frac{1}{r^2}\left(\boldsymbol{n_i}\cdot\boldsymbol{r_{ij}}\right)\left(\boldsymbol{n_j}\cdot\boldsymbol{r_{ji}}\right)\right\} \tag{6}$$

where $C(>0)$ is an interaction constant. Here, a new variable ϵ, which designates the anisotropic intermolecular interaction, is introduced into Equation (6) and gives

$$g_v\left(\boldsymbol{n_i},\boldsymbol{n_j},\boldsymbol{r_{ij}}\right) = \frac{C}{r^3}\left\{\boldsymbol{n_i}\cdot\boldsymbol{n_j} - 3\frac{\epsilon}{r^2}\left(\boldsymbol{n_i}\cdot\boldsymbol{r_{ij}}\right)\left(\boldsymbol{n_j}\cdot\boldsymbol{r_{ji}}\right)\right\} \tag{7}$$

The variable ϵ satisfies the following equation: $0 \leqq \epsilon \leqq 1$[20,21]. With this variable, the equation represents different degrees of nematic or anisotropic interactions between electric dipole moment vectors. Specifically, $\epsilon = 1$ means that molecules are subject to dipole-dipole interactions. When $\epsilon = 0$, the molecules follow the Maier-Saupe interaction law[18], which means that the molecular interactions are independent of the dipolar orientations. The variable ϵ is an indicator of dependence. The greater the value, the stronger the dependence of a molecule on others. When $\epsilon = 0$, each molecule behaves independently. In this study, the absolute value of g_v has no definite significance. Since we are concerned about the ratios between different molecules, it is sufficient to define $C = 1$. Consequently,

$$g_v\left(\boldsymbol{n_i}, \boldsymbol{n_j}, \boldsymbol{r_{ij}}\right) = \frac{1}{r^3}\left\{\boldsymbol{n_i} \cdot \boldsymbol{n_j} - 3\frac{\epsilon}{r^2}\left(\boldsymbol{n_i} \cdot \boldsymbol{r_{ij}}\right)\left(\boldsymbol{n_j} \cdot \boldsymbol{r_{ji}}\right)\right\} \tag{8}$$

By summing up the energy contributions from other molecules of the system, the energy state for molecule i can be expressed as

$$g_i = \sum_{i \neq j} \frac{1}{r^3}\left\{\boldsymbol{n_i} \cdot \boldsymbol{n_j} - 3\frac{\epsilon}{r^2}\left(\boldsymbol{n_i} \cdot \boldsymbol{r_{ij}}\right)\left(\boldsymbol{n_j} \cdot \boldsymbol{r_{ji}}\right)\right\} \tag{9}$$

The larger the value of g_i, the greater the attraction to the group. On the other hand, the smaller the value, the greater the repulsion.

Introducing anisotropic factor ϵ into the potential energy equation yields Equation (9), which describes the interaction-induced potential energy that molecule i has in the nematic state. Equation (9) represents the energy state of molecule i interacting with other molecules in the system.

Measurements of System Collective Orderliness Using Integrated Information Theory

This section describes the IIT metrics used to represent the collective orderliness of a system. First, we explain that axioms of the IIT, which postulate that information is integrated within a network. Next, we provide a mathematical description of the theoretical framework, and defines the complex (Φ) metric, which represents the amount of integrated information. Finally, we explain that the Φ metric represents the internal cause-effect relationship and consequently, denotes the collective orderliness of a system.

Integrated Information Theory: Approach to Quantitatively Characterize Consciousness

IIT provides a framework to infer the internal state of a system that cannot be observed on the basis of generally accepted axioms[22]. One major goal of this theory is to infer the quantity and quality of consciousness. Attempts have been made to apply IIT methodologies to the state of a clinically vegetative patient and quantitatively determine the level of consciousness. IIT presupposes several axioms, or essential properties, of consciousness.

First, IIT assumes that consciousness is informative, which leads to the notion of "intrinsic information" that is independent of an external observer. For example, thermometers have no intrinsic information. Thermometers provide information about the temperature, but they do not provide relevant information to the observers who need information on other properties such as atmospheric pressure and humidity. Because the quality of information that thermometers provide depends on the observer, they have no intrinsic information, and hence no experience or consciousness. Intrinsic information is quantitatively defined as the distance between the probability distributions of past states that are either constrained or unconstrained by the current state.

Second, IIT premises that consciousness is integrated. For example, a camera can store multiple pictures inside, but this does not mean that it has consciousness. The camera keeps such pictures independent of each other, whereas human beings can sort them based on their similarities by integrating the information of the pictures.

So far, we have discussed the two major presuppositions of the IIT theory: consciousness is informative and generates integrated intrinsic information. However, these characteristics alone do not necessarily indicate the presence of a boundary in consciousness that makes every experience definite. The IIT claims that consciousness is exclusive. This means that consciousness specifies only the maxima of integrated information. For example, the corpus callosum connects the right and left hemispheres in a healthy brain, and information processed separately in the respective hemispheres does not surface into consciousness in isolation from each other. However, in patients with epilepsy who underwent callosotomy, the right and left hemispheres process information independently. The split brains rarely cause split personality disorders because the more significant information comes to consciousness, as described by the exclusion axiom. A local maximum of integrated information is called a "complex." Currently, clinical attempts are being made to determine complexes. Following a concise presentation of the IIT theory of consciousness[23], we now turn to the mathematical aspects of the theory.

Mathematical Model of Integrated Information

IIT provides a mathematical model for system S based on a discrete-time multivariate stochastic process[24,25]

$$p\left(X_0, X_{\Delta t}, \ldots, X_t, X_{t+\Delta t}, \ldots, X_T\right) \tag{10}$$

Equation (10) satisfies the Markov property of Equation (11)

$$p\left(X_0, X_{\Delta t}, \ldots, X_t, X_{t+\Delta t}, \ldots, X_T\right) = p\left(X_0\right) \prod_{t=\Delta t}^{T} p\left(X_t | X_{t-\Delta t}\right) \tag{11}$$

This discrete dynamic system S is defined by a directed graph of interconnected nodes (a complete graph in this study) and its transition probability matrix (TPM). The TPM defines the conditional probability distribution: $p(X_t|X_{t-\Delta t})$. State vector X_t is composed of binary variables: $x_{t_i}, i = 1, 2, \ldots, n (n \in N)$. The joint probability distribution $p_{cause-effect}$ is defined as

$$p_{\text{cause - effect}}\ \left(X_{t-\Delta t}, X_t\right) := p_u\left(X_{t-\Delta t}\right) p_{\text{effect}}\ \left(X_t | X_{t-\Delta t}\right) \tag{12}$$

The marginal probability distribution $p_u(X_{t-\Delta t})$ is a uniform distribution that maximizes entropy distribution. From the above joint probability distribution are derived the transition probability distribution of the cause

$$p_{\text{cause}}\left(X_{t-\Delta t} | X_t\right) := \frac{p_{\text{casue-effect}}\ \left(X_{t-\Delta t}, X_t\right)}{\sum_{X_{t-\Delta t}} p_{\text{casue- effect}}\ \left(X_{t-\Delta t}, X_t\right)} \tag{13}$$

and the transition probability distribution of the effect

$$p_{\text{effect}}\left(X_t | X_{t-\Delta t}\right) := p\left(X_t | X_{t-\Delta t}\right) \tag{14}$$

The distribution functions are called the cause repertoire and effect repertoire at state X_t, respectively. For the cause repertoire, the amount of information reduced relative to the pre-transition state is examined across all partitions of the purview of mechanism M of the system or its subsystem ($M \subseteq S$)[26] . The partition that creates the least difference is called the minimum information partition (MIP). The cause information for the MIP ϕ_{cause} is called the integrated cause information (15). The integrated effect information ϕ_{effect} is derived in a similar manner (16). The integrated cause-effect information $\phi_{cause-effect}$ at state X_t is equal to either the integrated cause information or integrated effect information, whichever is smaller (17).

$$\phi_{\text{cause}}\ := \min_{i \in I} \left\{ D\left(p_{\text{cause}}\ \| p^{(i)}_{\text{cause}}\ \right) \right\} \tag{15}$$

$$\phi_{\text{effect}}\ := \min_{i \in I} \left\{ D\left(p_{\text{effect}}\ \| p^{(i)}_{\text{effect}}\ \right) \right\} \tag{16}$$

$$\phi_{\text{cause - effect}}\ := \min\left\{\phi_{\text{effect}}\ , \phi_{\text{cause}}\ \right\} \tag{17}$$

For all possible purviews of a given mechanism, ϕ values are computed, and the cause and effect repertoires that generate the maximum values are termed the maximally irreducible cause repertoire (MIC) and maximally irreducible effect repertoire (MIE), respectively.

$$\phi^{\max}_{\text{cause}}\ := \max_{j \in C} \left\{ \phi^{j}_{\text{cause}}\ \right\}, \phi^{\max}_{\text{effect}}\ := \max_{j \in C} \left\{ \phi^{j}_{\text{effect}}\ \right\} \tag{18}$$

where $C = 2N - 1$. (In this study, the "cut-one" approximation is employed, where only $2N$ bipartitions are evaluated instead of severing a single node from the rest of $2N$ nodes within the network.)

A "concept" refers to the maximally irreducible cause-effect repertoire that a mechanism specifies and its associated value of integrated information $\phi_{cause-effect}$ (17). A concept is equivalent to either MIC or MIE, whichever is smaller. If $\phi^{\max}_{\text{cause - effect}}\ > 0$, the mechanism in question constitutes a concept.

$$\phi^{\max}_{\text{cause - effect}}\ := \min\left\{\phi^{\max}_{\text{cause}}\ , \quad \phi^{\max}_{\text{effect}}\ \right\} \tag{19}$$

Next, for all mechanisms within a system $M \in \mathcal{P}(\mathcal{S})$, where $P(S)$ is the power set of the subsystem nodes, concept values are determined. A cause-effect structure (CES) is a set of concepts specified by all the mechanisms of the

system. After cutting the connection from a source element to a target element, the distance between the conceptual structure of the whole intact system and that of the partitioned system is measured. The sum of these distances is called the integrated conceptual information Φ (Big Phi). This metric quantifies the irreducibility of the set of elements under a unidirectional partition between elements. Unidirectional bipartition, $P_{\rightarrow} = \left\{S^{(1)}; S^{(2)}\right\}$, designates a process to "cut" a subsystem into two subsets $S^{(1)}$ and $S^{(2)}$, and sever the edge from $S^{(1)}$ to $S^{(2)}$ (noise is introduced into the connections).

The value of CES for a subset of a system following a unidirectional cut, $C\left(S^{P\rightarrow}\right)$ is determined and compared with $C(S)$. This process is repeated for all subsets, and the partitioning method that minimizes Φ (MIP) is determined (20). The largest among the MIPs for all subsets of the system is called the maximally irreducible cause-effect structure (MICS), and the subsystem giving rise to it is called a complex (21). Φ is a measure for system level exclusion.

$$\Phi_{Pi} = \min_{P\rightarrow 0} D\left(C(S), C\left(S^{P\rightarrow}\right)\right) \tag{20}$$

$$\Phi^{max} = \max(\Phi_{Pi}) \tag{21}$$

Distance D between the two probability distributions is evaluated in terms of the Hamming distance by applying the earth mover's distance (Wasserstein distance)[27]. The Wasserstein distance quantifies the cost of transforming one probability distribution into another. Although the Kullback-Leibler (KL) divergence is often applied to determine the distance between two probability distributions, it yields infinity when two distributions are disjointed. On the other hand, the Wasserstein metric provides a meaningful and smooth representation of the distance between two probability distributions[28].

Collective Order Parameter

The IIT theory defines consciousness using complex (Φ), which represents a set of mechanisms within a system to generate a local maximum of the integrated conceptual information. Although the IIT approach was originally employed to study consciousness in a human system of information-processing mechanisms, it is applicable to a broader range of networks, including a social system comprised of multiple members. In such a situation, Φ represents integration or collectivity among the members of the system. Moreover, the value of Φ may represent the degree of collective orderliness and connectivity among the system members.

Based on these considerations, we employ the Φ metric as a measure of order among schooling fish. MI, transfer entropy, and other measures for overall information propagation have been used to investigate the collective orderliness of a system[29]. Movements of individual members are evaluated in terms of distance, orientation, and behavioral diversity. However, these variables merely reflect superficial information available to the observer. They do not provide insight into the self-organizing process. Analysis of the apparent collective behavior may not capture the fundamental principles that underlie the collective orderliness and integration of the system. The factors that promote group connectivity remain unidentified. In our study, we apply the conceptual framework of IIT and use the Φ metric as the order parameter to infer the degree of group connectivity and collective orderliness.

Results

Complex (Φ) in the Polar Nematic Model

Results of the Φ Computation

Figure 2 shows the Φ changes in the value of ϵ, an indicator of anisotropy. The relationship between the number of fish and Φ is drastically affected by ϵ. When the value of ϵ is small (i.e., $= 0.3$), Φ increases significantly for a system of 6 fish compared with a system of 5 fish. Specifically, when $\epsilon = 0.3$, the average value of Φ is 0.132 at $n = 5$, but it increases approximately 10 times to 1.062 at $n = 6$. When the ϵ value is large (i.e., $= 0.7$), the Φ values appear to be independent of the number of fish. For example, when $\epsilon = 0.7$, the average Φ values are 0.150 at $n = 2$ and 0.254 at $n = 7$. The average Φ value shows a two-fold increase for $n = 7$ compared with $n = 2$. However, it is unclear whether these results indicate an increasing trend of Φ because the standard deviations also increase considerably.

The average Φ values are smallest when the number of fish is three or four for all ϵ values. The smallest average Φ value is 0.042 for $n = 3$ and $\epsilon = 0.7$. The polar nematic model, which is expressed as Equation (9), indicates the energy state of individual fish depends on the distance from other fish but not their orientation when $\epsilon = 0$. When $\epsilon = 0$, Φ shows a large increase from $n = 6$ to $n = 7$. A value of $\epsilon = 1$ signifies that all fish are always aligned in the same direction. In this scenario, Φ shows a minor decrease from $n = 2$ to $n = 3$, and then increases gradually from $n = 3$ to $n = 7$.

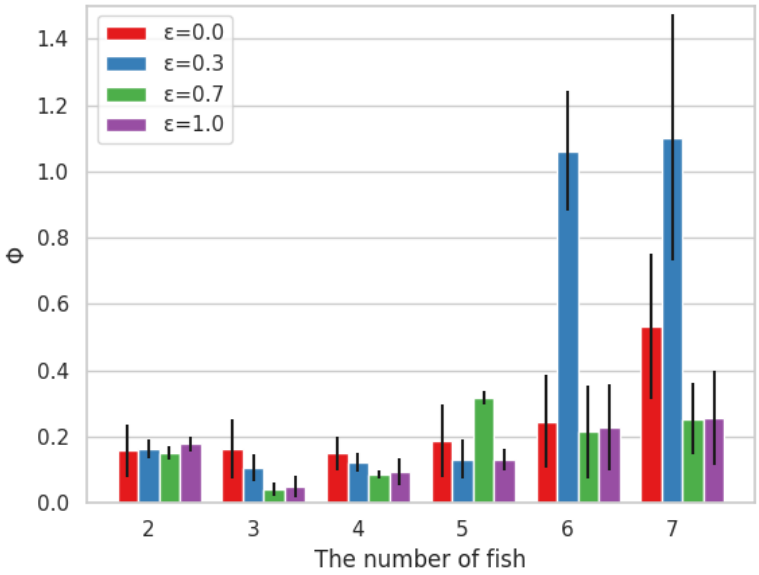

Figure 2. Relationship between the number of fish and Φ. Φ is the average of two samples. When ε=0.3, Φ increases in phase transition between 5 and 6 individuals.

Calculation of Φ Assuming Simple Inter-individual Interactions

In the polar nematic model, Φ drastically increases for $n = 6$ compared with $n = 5$ in the presence of a strong anisotropy (i.e., $\epsilon = 0.3$). In this section, Φ is determined considering three types of simple interactions presented in the literature[30,31]. In previous studies, isotropic models showed a marked increase in Φ when the number of system members increased from 3 to 4. Here Φ is calculated using a model similar to that presented in previous research to examine whether a disorder-to-order transition can occur in the absence of anisotropy. The difference between previous studies is that the transition probability matrix in this study is created using the logical conjunction ("AND") operation for processing inter-individual relationships. Similar to the section of complex(Φ) computation in the polar nematic model, the transition probability matrix is created from the absolute position data.

Results of Φ Computation

Figure 3 shows the results in a three-dimensional manner. Regardless of the threshold value, there is not a meaningful relationship when comparing the warm color spots (greater Φ values). The Φ values do not show a consistent trend with N. The Φ values are generally smaller for $N = 3$ compared with $N = 2$, but are larger for $N = 4$ than for $N = 3$. Φ has the greatest value (0.15) for $N = 2$ with a distance of $140mm$, field of view of 1.6π rad, and turning rate of 0π rad. The model based on simple interactions contradicts the polar nematic model, where Φ increases with the number of system members. In a previous study that employed a model similar to that presented in this section[32], Φ showed an abrupt increase when the sample size increased by one from a certain number, although the transition probability matrix was constructed in a different manner.

The Φ values are close to 0 when the distance threshold is $0mm$ for all N values. As the distance threshold increases, Φ gradually increases when $N = 2$ and Φ is nearly the same when the other N. As the field of view threshold increases, Φ also increases when N is equal to 2. For $N = 6$, Φ is the largest at 0.0π rad. For the other N, Φ is the largest at 0.4π rad. Φ is the greatest when the turning rate threshold is 0.0π rad for any number of fish investigated. As the turning rate threshold increases, Φ becomes small. As explained above, a consistent trend is not observed for the relationship between Φ and distance or field of view thresholds.

Comparison of Mutual Information and Φ

So far, we investigated the collective orderliness using the Φ metric, which quantifies the strength of all causal influences among the parts of a system. On the other hand, MI represents the upper limit of the total causal influences in the whole system. These two metrics follow the mathematical formula: MI $>$ Φ[26]. In this section, the changes in Φ and MI with the sample size and whether this relationship holds for the MI and Φ values obtained

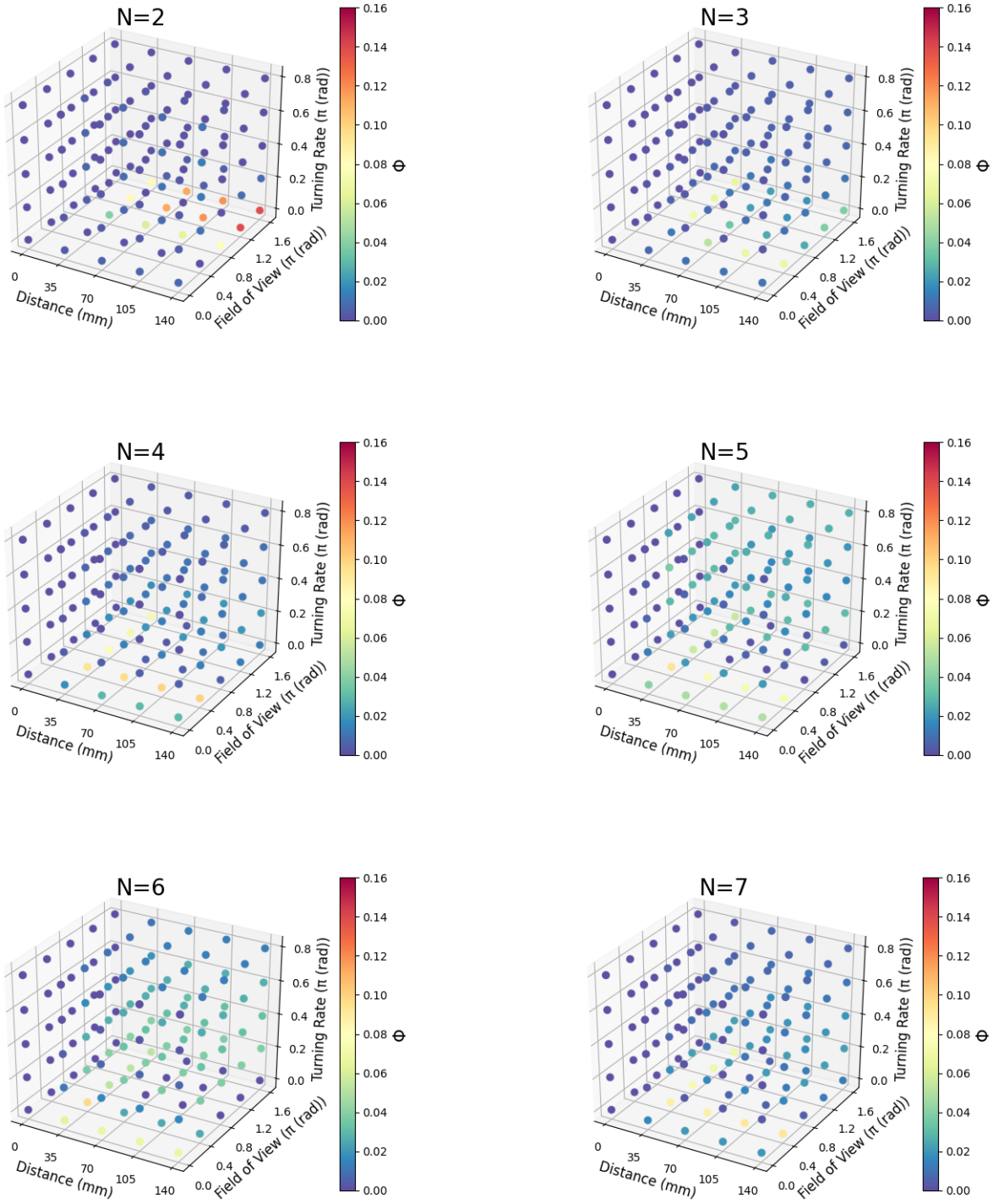

Figure 3. The heat map shows Φ. Each axis corresponds to a different parameter : Distance (mm), Field of View (π (rad)) and Turning Rate (π (rad)).

from our simulations are investigated.

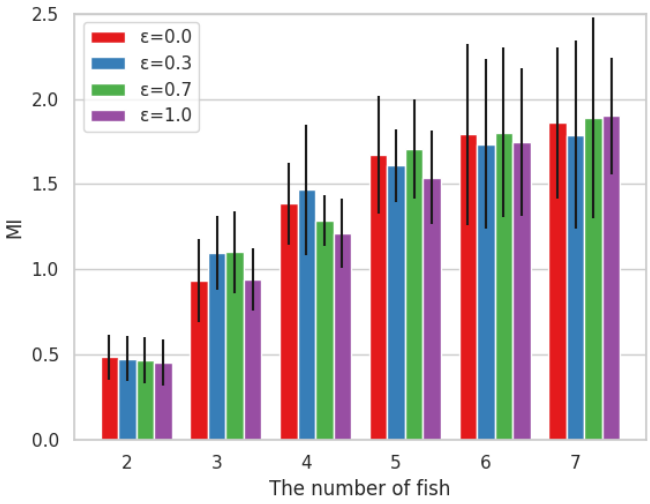

Figure 4. Relationship between the number of fish and MI. MI is the average of two samples. The standard deviation of MI is 0 except when the number of fish is two. MI increases with fish population.

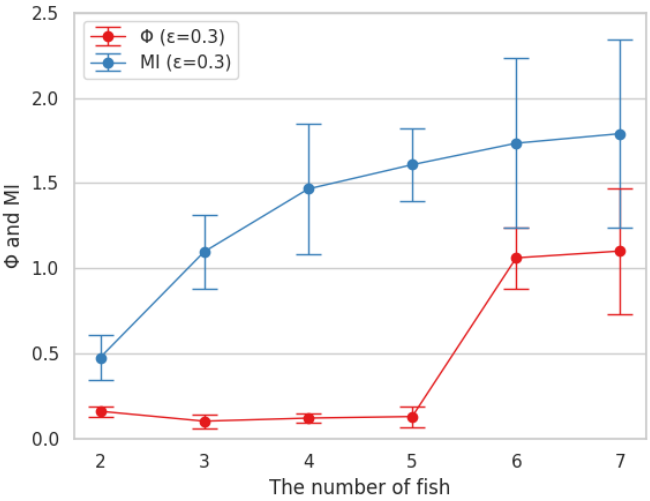

Figure 5. Relationship between MI and Φ due to the changes in population when $\varepsilon = 0.3$. MI is always higher than Φ.

Results of Mutual Information Computation

The MI values increase logarithmically with sample size (Figure 4). These results represent a logical consequence of increasing the sample size, which raises the level of disorderliness.

Figure 5 compares the MI values and the Φ values with an emphasis $\epsilon = 0.3$ because a drastic change in Φ between the five- and six-fish systems is observed. Φ is always smaller than MI. Our study provides experimental support for the mathematically proven formula: MI $>$ Φ[26].

Discussion

Our polar nematic model indicates that ϵ has a notable impact on the behavior of Φ by sample size. Specifically, when $\epsilon = 0.3$, Φ drastically increases as the number of fish increases from 5 to 6. This phenomenon is consistent with the phase transitions in active matter, which are well characterized by the Vicsek, boids, and other mathematical models. Our polar nematic model exhibits a striking difference from the simple-interaction model and MI model, which fail

to present the transitional dynamics in fish schooling. Our polar nematic model represents the non-equilibrium statistical physics of active matter when a strong anisotropy is assumed (i.e., $\epsilon = 0.3$ in the possible range of 0-1). Moreover, our study suggests that polar nematic models require the Φ metric as an order parameter to simulate disorder-to-order transition dynamics.

A previous study showed that leadership emerged in a fish school as Φ increases[30]. However, our experimental observations of the 5- and 6-fish groups did not identify any meaningful differences in the collective movement. This may suggest that the changes occurring between the 5- and 6-fish groups are not of an externally observable nature.

As shown in the section of assuming simple inter-individual interactions, the turning rate of 0 rad increases the Φ value greatly regardless of the sample size. However, the Φ values depend greatly on the distance and field of view thresholds, but a clear trend did not appear. Living organisms have receptors that respond to specific external stimuli. If Φ of a group of neon tetras increases greatly at a certain threshold, it may characterize the physiological role of a particular receptor in regulating collective behavior. However, our simulations did not identify parameter thresholds that provide new insight into the species' physiology of schooling behavior.

The observation that there is not a threshold for any of the three physiological parameters on Φ may indicate methodological flaws in our modeling or neon tetras' capabilities to respond to the full parameter ranges investigated. The previous study showed that these three parameters affect organisms that act in groups[4]. Neon tetras, which act in groups, would be no exception to this rule. Unlike the results of complex(Φ) computation, the Φ metric does not show a general increasing trend with the sample size. These results may suggest two mutually exclusive possibilities. 1) The proposed simple-interaction model is appropriately constructed, and Φ of the real-life groups of neon tetras is almost independent of size. 2) The proposed model is inappropriate, resulting in the wrong simulations. The second hypothesis was not investigated this time.

Based on the first hypothesis, the implications of Φ values remaining low regardless of the increase in the sample size is discussed in this reference[23]. Consider two networks of a small number of neurons as a simplified brain model. Model A consists of eight neurons, which are connected to the other ones by synapses. Model B has six neurons, which are not interconnected. Our interest is to determine which system has the greater Φ. Superficial reflections may lead one to consider that Model A has the greater Φ. Indeed, the MI, a metric for the amount of information in the entire system, is greater in Model A. However, Φ is greater for Model B because of the locally asymmetric nature of information transmission associated with disconnected neurons. A homogeneous network has less diversity in its information quality than an inhomogeneous network, which weakens the strength of all causal influences among its parts. Thus, Model B, which has a more diverse neural network, has a greater Φ than Model A.

This leads to the next topic, "Does network diversity increase Φ?" In a feed-forward neural network that transmits information unidirectionally, Φ is equal to 0 because the network does not allow for synchronous information sharing among neurons. Increasing the Φ value of a system requires network diversity and bidirectional connection between its elements. In light of the comparison of these simple neural network models, the small Φ values obtained for a group of neon tetras may suggest the absence of system diversity despite bidirectional information sharing among the members. System diversity refers to the varied characteristics and asymmetric interrelationships of the members. Loss of system diversity means order formation because the similarity among the members' behaviors reflects the loss of variation and asymmetry. When the members of a system start to act in subordination to others, the system develops a higher level of unity and becomes less diverse.

Several other reasons may account for the small Φ values. First, our experimental design may have prevented schooling behavior at the time of video recording. We frequently noticed during experiments that when one fish started moving around, others followed it. However, not all fish made coordinated schooling movements at a given time. The fish were often hovering or swimming alone. In a previous study, sweetfish (Plecoglossus altivelis) was used to determine Φ[30].

The results in the section of mutual information computation demonstrate that the theoretically proven relationship of MI $>$ Φ is valid for all sample sizes investigated. These results validate the Φ computations shown in the section of complex(Φ) computation in the polar nematic model. Moreover, these results support the legitimacy of the phase transition-like behavior of the Φ metric, which is substantiated by a drastic change observed for $\epsilon = 0.3$.

Methods

Experimental Procedures

Video Recording

Immediately before the experiment, a predetermined number of healthy neon tetras were randomly selected and transferred from the aquarium to a water-filled petri dish (diameter: $140mm$). After the fish acclimated to the environment for several minutes and their behaviors stabilized, a tablet computer (iPad Pro Third Generation) was

Table 1. Example of transition probability matrix (TPM) when N = 2. The matrix is in state-by-node form, assuming conditional independence, where state is the 2^N state and node is the N element . Information loss occurs due to the conversion from state-by-state to state-by-node. Since the size of state-by-state is $2^N \times 2^N$, conversion to state-by-node reduces the number of elements and the amount of information . Therefore, the probability distributions when the state is at time t and at time t + 1 are given independently

State at t	Pr(N=ON) at t+1	
(A, B)	A	B
(0, 0)	0.7	0.6
(1, 0)	0.3	0.1
(0, 1)	0.9	0.4
(1, 1)	0.5	0.2

placed 23cm above and parallel to the laboratory bench surface to record video of the fish behavior. The petri dish and tablet camera were covered with a sheet of thin paper rolled to form a cylinder-shaped shield to minimize distraction by moving objects in the laboratory and to prevent reflection of light on the water surface. As soon as the experimental setup was ready, 1,080-pixel resolution video was recorded at a rate of 30 frames per second using the default software.

Fish Tracking and Acquisition of Position Time Series Data

The open source UMAtracker software was used to track each fish[33]. This program automatically distinguished and tracked individual fish by applying special filters. If automated tracking was lost in a frame, corrections were made manually (Figure 6). The duration of one recording session was 15 minutes based on the consideration that a longer time frame may allow the fish to reduce vigilance and eventually stop grouping behaviors. Preliminary experiments showed no noteworthy changes in the integrated information metrics during 15-minute sessions.

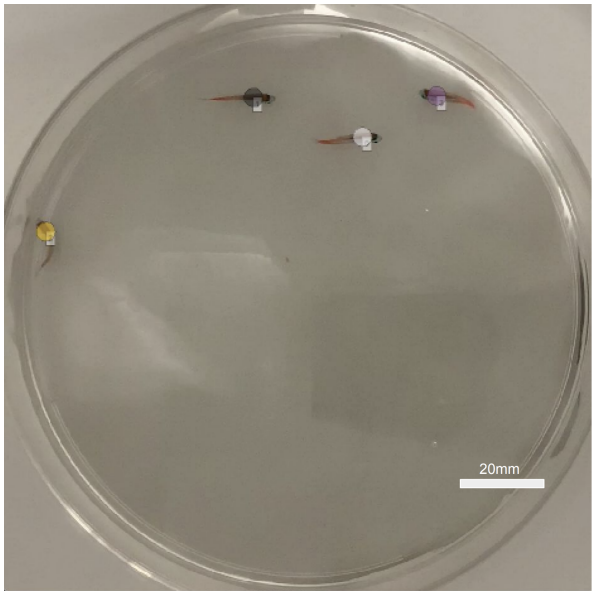

Figure 6. Tracking each fish using UMATracker[33].

Position Time Series Analysis

First, noise was removed by taking a moving average of five consecutive time-series data, and the data were further aggregated into 1/6−second intervals. This interval was taken from a previous study that evaluated fish's reaction time from a sensory input to an appropriate behavioral response[29].

Application of the Polar Nematic Model

Position time series data were substituted into the polar nematic model (9) to give time series data of the state of individual fish, which were termed "time series state vectors." The values derived from Equation (9) had dimensions of energy, and were either positive or negative. Larger and smaller values indicated greater and weaker intra-system connectivity, respectively. In Equation (9), only the hyperparameter ϵ is a variable. Many models in the literature include multiple variable parameters[34], whereas this study investigates the effects of one parameter. Due to restrictions on the computational capacity, the following discrete values were used for $\epsilon : 0, 0.3, 0.7$, and 1.

Transition Probability Matrix

Each element of the time series state vector was assumed to be a stochastic value in the range of -1 to 1, while the cognitive state of an organism was assumed to be binary. Because the cognitive state was either ON $(= 1)$ or OFF $(= 0)$, each vector element was represented as the probability of taking the ON state. Elements with negative values represent negative probabilities (quasi-probabilities), indicating the "unlikeliness" of taking the ON state. Based on the numbers of possible transitions and time series state vectors for individual fish, a matrix was created and normalized to yield the transition probability matrix.

The procedure to formulate the transition probability matrix is explained in reference to Table 1, which provides data for a system comprised of two fish. The two fish, labeled A and B, can individually take either the ON or OFF state. Hence, there are 2^2 $(= 4)$ possible states for the system. The state vector determined for a given time [in the form of (α, β), where α and β indicate the probability for fish A and B to be in the ON state, respectively] indicates the existence probabilities for each of the four possible states. For example, the state vector for time t $(0.3, 0.8)$ indicates that the probability vector for the system to take state [A $= 0$, B $= 0$] is $(0.7, 0.2)$ and the probability vector for the system to take state [1, 0] is $(0.3, 0.2)$. The probability vectors for the system to take states [0, 1] and [1, 1] are determined in a similar manner. Assuming that the state vector for time $t + 1$ is $(0.6, 0.7)$, the probability vector for the system to transition from state [0, 0] at time t to state [1,1] at time $t + 1$ is $(0.7 \times 0.6, 0.2 \times 0.7)$ because the existence probabilities for state [0, 0] at time t are $(0.7, 0.2)$.

Similarly, the probabilities of transitioning from states [1,0], [0,1], and [1,1] at time t to state [1,1] at time $t + 1$ were determined. Thus, eight matrix elements denoted the transition from the four possible states at time t to state [1,1] at time $t + 1$. This procedure was repeated for all combinations from time t to time $t + 1$, and the resulting respective matrix elements were added and processed to represent the probabilities. This means that each element was normalized to the range of 0 to 1. More specifically, the greatest matrix element value was converted to unity $(= 1)$, whereas the minimum value was converted to zero $(= 0)$. The intermediate values were converted appropriately to fall within the range. The column-wise sum of elements for any time t did not have to equal unity because conditional independence is assumed for time series data. Table 1 shows the transition probability matrix determined for the mathematical procedures described above.

Computation of Each Amount of Information

Computation of Complex (Φ) Based on Polar Nematic Model

Complex (Φ) was calculated using the Pyphi software package[35]. Pyphi is used to compute integrated information, complexes, concepts, and other IIT metrics. The program was used to determine the Φ values for each state of the system. In the case of a system comprised of two fish, Φ was determine for each of the $2^2(= 4)$ states. The Pyphi's cut-one approximation option was selected to compute the Φ values to enable parallel processing. Moreover, high-speed processing methods were used to evaluate the polar nematic state equations. Despite these efforts, the computational requirements were so demanding[36] that seven was the highest number of fish in this study.

Since the Φ values did not change notably for any group of fish throughout the measurements, the Φ values averaged over the entire time series was taken as the representative Φ for the group.

Computation of Φ Based on Simple Inter-individual Relationships

The ON-OFF state was determined for individual fish. The ON state means that the fish in question is interacting with one or more of the others of the system. The ON state required three conditions to be met. First, the distance between the fish in question and its nearest neighbor must be below a certain threshold (distance). This requirement takes the bidirectional nature of the interactions into account. Second, at least one fish must be present within the predetermined visual field (angle) of the individual in question (field of view). Unlike the first requirement, this takes into account the asymmetric nature of the interactions. Third, the turning rate of the individual in question must be equal to or greater than a given threshold (turning rate).

The current ON state of the fish in question affects the state of the others at the next time point. The significance of the turning behavior has experimentally and theoretically been shown to affect the collective behavior of animal

groups[37]. Here, the fish in question was defined to be ON when all three conditions were satisfied. That is, this model performed a logical product ("AND") operation for the three conditions. For example, if the distance condition was ON (= true), field of view condition was OFF (= false), and turning rate condition was ON (= true), then the individual was in the OFF state. The ON-OFF state at time t was determined for n individuals ($n = 2 - 6$). By using binary variables 1 and 0 to denote the ON and OFF states, respectively, a state vector provided either 0 or 1 for the state of the system at time t. The ON-OFF state was determined for each condition as described below.

1. Distance Condition

The distance between the fish in question i and another fish j at time t is determined from their absolute position time data. A set of individuals that are within a threshold distance ζ from the fish in question can be expressed as

$$S_i^t = \{j | d(\boldsymbol{x}_i(t), \boldsymbol{x}_j(t)) < \zeta, j \neq i\} \tag{22}$$

where $\boldsymbol{x_i}(t)$ denotes the absolute position coordinates of the fish in question i at time t , and $d(\boldsymbol{x}, \boldsymbol{y})$ denotes the Euclidean distance between$\boldsymbol{x}$ and $\boldsymbol{y}$. The ON-OFF function based on the distance condition can be shown as: $(D_i^t(\boldsymbol{x}_1(t), \boldsymbol{x}_2(t), \cdots, \boldsymbol{x}_n(t)) : \mathbb{R}^d \times \mathbb{R}^d \times \cdots \times \mathbb{R}^d \to \{0, 1\}$. When |S| is defined to designate the number of individuals in set S, $D_i^t(\boldsymbol{x}_1(t), \boldsymbol{x}_2(t), \ldots, \boldsymbol{x}_n(t))$ equals to 1 for $|S_i^t| > 0$. Otherwise, it is 0.

2. Field of View Condition

The set O_i^t includes individuals that are located within the threshold visual angle η of the fish in question i at time t

$$O_i^t = \{j | \arg(\boldsymbol{v}_i(t), \boldsymbol{v}_j(t)) < \eta, j \neq i\} \tag{23}$$

where $\boldsymbol{v}_i(t)$ designates the velocity vector of the fish in question i at time t, which is determined based on the difference between the absolute position coordinates $\boldsymbol{x}_i(t)$, at time t and $\boldsymbol{x}_i(t-1)$ at time $t-1$. The term $\arg(\boldsymbol{v}_1(t)$ $\boldsymbol{v}_2(t))$ provides the angle of two vectors. The ON-OFF function for the field of view condition can be expressed as $B_i^t(\boldsymbol{v}_1(t), \boldsymbol{v}_2(t), \cdots, \boldsymbol{v}_n(t)) : \mathbb{R}^d \times \mathbb{R}^d \times \cdots \times \mathbb{R}^d$ When $|O_i^t|$ denotes the number of individuals included in set O_i^t, then $B_i^t(\boldsymbol{v}_1(t), \boldsymbol{v}_2(t), \cdots, \boldsymbol{v}_n(t))$ is equal to 1 for $|O_i^t| > 0$. Otherwise, it is 0.

3. Turning Rate Condition

The ON-OFF function for the turning rate condition of the fish in question i at time t is given as:$T_i^t(\boldsymbol{v}_i(t), \boldsymbol{v}_i(t - \Delta t))$: $\mathbb{R}^d \times \mathbb{R}^d \to \{0, 1\}$,$\boldsymbol{v}_i(t)$ designates the velocity vector of the fish in question i at time t. $\boldsymbol{v}_i(t)$ can be determined from the difference between the position coordinates at time t and time $t-1$. The function is 1 when the turning rate is equal to or greater than the threshold beginmathδ. Specifically, when $\arg(\boldsymbol{v}_i(t), \boldsymbol{v}_i(t - \Delta t)) \geq \delta$, then $T_i^t(\boldsymbol{v}_i(t), \boldsymbol{v}_i(t - \Delta t))$ is 1. Otherwise, it is 0.

The following term is derived for fish i at time t as the logical product of the three functions for the distance, field of view, and turning rate conditions

$$D_i^t(\boldsymbol{x}_1(t), \boldsymbol{x}_2(t), \cdots, \boldsymbol{x}_n(t)) \wedge B_i^t(\boldsymbol{v}_1(t), \boldsymbol{v}_2(t), \cdots, \boldsymbol{v}_n(t)) \wedge T_i^t(\boldsymbol{v}_i(t), \boldsymbol{v}_i(t - \Delta t)) \tag{24}$$

The logical product is expressed as: $\wedge : \{0, 1\}^2 \to \{0, 1\}$. The value is equal to 1 for $1 \wedge 1$. Otherwise, it is 0. The state of the fish i at time t is denoted using the threshold matrix (ζ, η, δ) as: $s_i(t; \zeta, \eta, \delta) \in \{0, 1\}$. The state vector for the system at time t is given as: $s(t) = (s_1(t), s_2(t), \ldots, s_n(t)) \in \{0, 1\}^n$. The threshold parameters are not shown in the equation for the sake of simplicity.

The state vector created in the section of complex(Φ) computation in the polar nematic model contains stochastic variables, whereas the state vector created in this section contains Boolean variables (0 and 1). Unlike the procedures in the section of complex(Φ) computation in the polar nematic model, the existence probabilities can be neglected in the transition probability matrix here. The matrix was constructed based on the numbers of possible transitions for each fish and normalizing the matrix elements. In a previous study, the transition probability matrix was created using the logical product operation to process inter-individual relationships[30]. According to their approach, the fish in question could not take the ON state unless all other members of the system were in the ON state in the previous time point. Thought experiments suggest that this assumption is not acceptable. Consider a group of five fish, and assume that among the four individuals other than the fish in question, one is OFF and three are ON at a given time. According to their model, the fish in question will take the OFF state at the subsequent

time point. However, it is very unlikely that the influence from one OFF individual exceeds that from three ON individuals. Instead of a deterministic methodology, our approach explores the mechanism of group dynamics based on experimental data. In other words, we adopted a phenomenological approach to investigate the intersubjective dynamics of fish schooling. The IIT methodology, which addresses intrinsic information that is not reducible to directly measurable metrics, allows unknown relationships within a system to be inferred based on measurement data. Using the resulting transition probability matrix, we determined the Φ values for each possible state of the system. These values were then averaged over the entire time series to yield the system's Φ value, an indicator for system collective consciousness.

Computation of Mutual Information

Using the polar nematic model, we calculated MI using the time series state vector. The state vector at time t and time $t, t-\Delta t$ can be shown using binary variables as and , respectively, where N represents the number of state vector elements. The MI for the two variables $X_t = (x_1^t, x_2^t, ..., x_N^t)$ and $X_{t-\Delta t} = (x_1^{t-\Delta t}, x_2^{t-\Delta t}, ..., x_N^{t-\Delta t})$ is

$$\begin{aligned} \min_{q(X_t, X_{t-\Delta t})} D_{KL}[p\|q] &= \sum_{X_t, X_{t-\Delta t}} p\left(X_t, X_{t-\Delta t}\right) \log \frac{p\left(X_t, X_{t-\Delta t}\right)}{p\left(X_t\right) p\left(X_{t-\Delta t}\right)} \\ &= H\left(X_t\right) + H\left(X_{t-\Delta t}\right) - H\left(X_{t-\Delta t} | X_t\right) \\ &= I\left(X_t; X_{t-\Delta t}\right) \end{aligned} \tag{25}$$

The MI was computed for each time point, and the mean value, which was averaged across all time points, was defined as the system's MI.

References

1. Camazine, S. *et al. Self-organization in biological systems*, vol. 7 (Princeton university press, 2003).
2. Cavagna, A., Queirós, S. D., Giardina, I., Stefanini, F. & Viale, M. Diffusion of individual birds in starling flocks. *Proc. Royal Soc. B: Biol. Sci.* **280**, 20122484 (2013).
3. Couzin, I. D. *et al.* Uninformed individuals promote democratic consensus in animal groups. *science* **334**, 1578–1580 (2011).
4. Reynolds, C. W. Flocks, herds and schools: A distributed behavioral model. *SIGGRAPH Comput. Graph.* **21**, 25–34, https://doi.org/10.1145/37402.37406 (1987).
5. Hashimoto, M., Gotoh, H., Harada, E. & Sakai, T. Development of numerical fishway by fish-school boids. *PROCEEDINGS OF HYDRAULIC ENGINEERING* **49**, 1477–1482 (2005).
6. Berthier, L. & Kurchan, J. Non-equilibrium glass transitions in driven and active matter. *Nat. Phys.* **9**, 310–314 (2013).
7. Marchetti, M. C. *et al.* Hydrodynamics of soft active matter. *Rev. Mod. Phys.* **85**, 1143 (2013).
8. Ginelli, F. The physics of the vicsek model. *The Eur. Phys. J. Special Top.* **225**, 2099–2117, https://doi.org/10.1140/epjst/e2016-60066-8 (2016).
9. Vicsek, T., Czirók, A., Ben-Jacob, E., Cohen, I. & Shochet, O. Novel type of phase transition in a system of self-driven particles. *Phys. Rev. Lett.* **75**, 1226–1229, https://doi.org/10.1103/PhysRevLett.75.1226 (1995).
10. Kawaguchi, K., Kageyama, R. & Sano, M. Topological defects control collective dynamics in neural progenitor cell cultures. *Nature* **545**, 327–331 (2017).
11. Ballerini, M. *et al.* Interaction ruling animal collective behavior depends on topological rather than metric distance: Evidence from a field study. *Proc. Natl. Acad. Sci.* **105**, 1232–1237, http://doi.org/10.1073/pnas.0711437105 (2008).
12. Cavagna, A. *et al.* Flocking and turning: a new model for self-organized collective motion. *J. Stat. Phys.* **158**, 601–627 (2015).
13. Attanasi, A. *et al.* Information transfer and behavioural inertia in starling flocks. *Nat. physics* **10**, 691–696 (2014).
14. Wicks, R. T., Chapman, S. C. & Dendy, R. O. Mutual information as a tool for identifying phase transitions in dynamical complex systems with limited data. *Phys. Rev. E* **75**, 051125, https://doi.org/10.1103/PhysRevE.75.051125 (2007).

15. Albantakis, L. & Tononi, G. The intrinsic cause-effect power of discrete dynamical systems—from elementary cellular automata to adapting animats. *Entropy* **17**, 5472–5502 (2015).

16. Toner, J. & Nelson, D. R. Smectic, cholesteric, and rayleigh-benard order in two dimensions. *Phys. Rev. B* **23**, 316 (1981).

17. Küpfer, J. & Finkelmann, H. Nematic liquid single crystal elastomers. *Die Makromolekulare Chemie, Rapid Commun.* **12**, 717–726 (1991).

18. Barbero, G. & Evangelista, L. *An Elementary Course on the Continuum Theory for Nematic Liquid Crystals.* Series on Liquid Crystals (World Scientific Publishing Company, 2000).

19. Sunakawa, S. *Electromagnetism.* No. 4 in physics text series (Iwanami Shoten, 1987).

20. Skačej, G., Pergamenshchik, V., Alexe-Ionescu, A., Barbero, G. & Žumer, S. Subsurface deformations in nematic liquid crystals: The hexagonal lattice approach. *Phys. Rev. E* **56**, 571 (1997).

21. Bradač, Z., Kralj, S. & Žumer, S. Molecular dynamics study of nematic structures confined to a cylindrical cavity. *Phys. Rev. E* **58**, 7447 (1998).

22. Oizumi, M., Albantakis, L. & Tononi, G. From the phenomenology to the mechanisms of consciousness: integrated information theory 3.0. *PLoS Comput. Biol* **10**, e1003588 (2014).

23. Massimini, M. & Tononi, G. *When consciousness is born: Integrated information theory to challenge the mysteries of the brain. Tomoko Hanamoto, trans.* (Aki Shobo, 2015).

24. Barrett, A. B. & Seth, A. K. Practical measures of integrated information for time-series data. *PLoS computational biology* **7** (2011).

25. Oizumi, M., Amari, S.-i., Yanagawa, T., Fujii, N. & Tsuchiya, N. Measuring integrated information from the decoding perspective. *PLoS computational biology* **12** (2016).

26. Oizumi, M., Tsuchiya, N. & Amari, S.-i. Unified framework for information integration based on information geometry. *Proc. Natl. Acad. Sci.* **113**, 14817–14822 (2016).

27. Tegmark, M. Improved measures of integrated information. *PLoS computational biology* **12** (2016).

28. Arjovsky, M., Chintala, S. & Bottou, L. Wasserstein generative adversarial networks. In *Proceedings of the 34th International Conference on Machine Learning - Volume 70*, ICML'17, 214–223 (JMLR.org, 2017).

29. Crosato, E. *et al.* Informative and misinformative interactions in a school of fish. *Swarm Intell.* **12**, 283–305 (2018).

30. Niizato, T. *et al.* Finding continuity and discontinuity in fish schools via integrated information theory. *PLOS ONE* **15**, e0229573, (2020).

31. Niizato, T. *et al.* New classification of collective animal behaviour as an autonomous system, https://doi.org/10.20944/preprints201902.0269.v1 (2019).

32. Niizato, T. *et al.* Different collective behaviors in different small schools of plecoglossus altivelis. *Transactions Soc. Instrum. Control. Eng.* **52**, 257–263 (2016).

33. Yamanaka, O. & Takeuchi, R. Umatracker: an intuitive image-based tracking platform. *J. Exp. Biol.* **221** (2018).

34. Johansson, A., Helbing, D. & Shukla, P. K. Specification of the social force pedestrian model by evolutionary adjustment to video tracking data. *Adv. complex systems* **10**, 271–288 (2007).

35. Mayner, W. *et al.* Pyphi: A toolbox for integrated information theory. *PLOS Comput. Biol.* **14**, (2017).

36. Nilsen, A., Juel, B. & Marshall, W. Evaluating approximations and heuristic measures of integrated information. *Entropy* **21**, 525, (2019).

37. Couzin, I. D., Krause, J., James, R., Ruxton, G. D. & Franks, N. R. Collective memory and spatial sorting in animal groups. *J. theoretical biology* **218**, 1–12 (2002).

Acknowledgements

This study was supported by MEXT KAKENHI (Grant Number 15H05861).

Author contributions statement

S.W. and Y.I.: conception, design of the study; S.W. and Y.M.: performed experiments and data analysis; S.W., K.M. and Y.I: interpretation; S.W. drafted manuscript. All authors reviewed the manuscript.

Additional information

Competing interests The authors declare no competing interests.